NUMERICAL ANALYSIS OF CLASSICAL AND INVERSE PROBLEMS OF DETONATION

K. Jach

UDC 532.59

The phenomenon of the formation of a detonation jet is well known. However, this process is so complex that it will long be the subject of continued investigation. The present study is of a theoretical nature. The results reported here were obtained by a numerical method which may prove useful in the study of detonation phenomena.

The first theories of the formation of a detonation jet were proposed by Lavrent'ev [1] and, independently, by Birghoff et al. [2]. This theory was later examined by several scientists and was augmented by new elements (allowance for the elastoplastic properties of the material, inverse detonation, etc.) [3-6]. The development of numerical methods opened up new possibilities for studying detonation processes. These methods can be used in an attempt to solve the general problem of a two-dimensional unsteady process. The first two-dimensional calculations of a detonation process were performed in [7]. The study [8] offered an example of a calculation in which allowance is made for the effect of the propagation of the detonation wave from an explosive on the lining of a shaped charge. Here, we performed numerical experiments by an original method developed at the Institute of Plasma Physics and Laser Microsynthesis.

Physical–Mathematical Formulation of the Problem. Figure 1 shows the general scheme of the shaped charge. The behavior of the explosive and the lining can be described by the following system of equations [9, 10]:

$$\frac{d\rho}{dt} + \rho \operatorname{div} \mathbf{w} = 0,$$

$$\rho \frac{du}{dt} = -\frac{\partial p}{\partial r} + \frac{\partial S_{rr}}{\partial r} + \frac{\partial S_{rz}}{\partial z} + \frac{S_{rr} - S_{\theta\theta}}{r},$$

$$\rho \frac{dv}{dt} = -\frac{\partial p}{\partial z} + \frac{\partial S_{rz}}{\partial r} + \frac{\partial S_{zz}}{\partial z} + \frac{S_{rz}}{r},$$

$$\rho \frac{d\varepsilon}{dt} = -p \operatorname{div} \mathbf{w} + S_{rr} \frac{\partial u}{\partial r} + S_{\theta\theta} \frac{u}{r} + S_{zz} \frac{\partial v}{\partial z} + S_{rz}\left(\frac{\partial u}{\partial z} + \frac{\partial v}{\partial r}\right),$$

$$\frac{dS_{rr}}{dt} = 2\mu\left(\frac{\partial u}{\partial r} - \frac{1}{3} \operatorname{div} \mathbf{w}\right) - \left(\frac{\partial u}{\partial z} - \frac{\partial v}{\partial r}\right) S_{rz},$$

$$\frac{dS_{\theta\theta}}{dt} = 2\mu\left(\frac{u}{r} - \frac{1}{3} \operatorname{div} \mathbf{w}\right),$$

$$\frac{dS_{zz}}{dt} = 2\mu\left(\frac{\partial v}{\partial z} - \frac{1}{3} \operatorname{div} \mathbf{w}\right) + \left(\frac{\partial u}{\partial z} - \frac{\partial v}{\partial r}\right) S_{rz},$$

$$\frac{dS_{rz}}{dt} = \mu\left(\frac{\partial u}{\partial z} + \frac{\partial v}{\partial r}\right) + \frac{1}{2}\left(\frac{\partial u}{\partial z} - \frac{\partial v}{\partial r}\right)(S_{rr} - S_{zz}),$$

where div w = (∂u/∂r) + (∂v/∂r) + (u/z); u and v are projections of the velocity vector on the r and z axes, respectively; ρ is density; p is pressure; ε is the internal energy; S_{ik} are components of the deviatoric part of the stress tensor (S_{ik} = 0 for the explosive). The equations of state for the copper lining [7]

$$p = \left\{a + b\left[\frac{\varepsilon}{\varepsilon_0}\left(\frac{\rho_0}{\rho}\right)^2 - 1\right]^{-1}\right\}\rho\varepsilon + A\left(\frac{\rho}{\rho_0} - 1\right) + B\left(\frac{\rho}{\rho_0} - 1\right)^2,$$

and the explosive [11]

$$p = C\rho^3 + D\rho\varepsilon.$$

We adopted the von Mises criterion, with reduction to a yield circle, to describe plastic flow

$$2I = S_{zz}^2 + S_{rr}^2 + S_{\theta\theta}^2 + 2S_{rz}^2 \leqslant \frac{2}{3} Y^2 \qquad (1)$$

Warsaw. Translated from Zhurnal Prikladnoi Mekhaniki i Tekhnicheskoi Fiziki, No. 2, pp. 123-129, March-April, 1987. Original article submitted November 29, 1985.

0021-8944/87/2802-0277$12.50

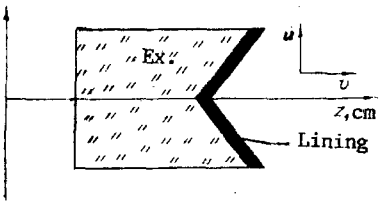

Fig. 1

(Y is the dynamic yield point). If condition (1) is violated, then the components S_{ik} are multiplied by $(\sqrt{2}\ Y/3)/2I$. The fracture of the lining material was described in accordance with the conditions [12]

$$\delta = \rho/\rho_0,$$

$$F(\delta) = \begin{cases} 1 & \text{for} \quad \delta > \delta_1, \\ \dfrac{\delta - \delta_2}{\delta_1 - \delta_2} & \text{for} \quad \delta_2 < \delta \leqslant \delta_1, \\ 0 & \text{for} \quad \delta \leqslant \delta_2, \end{cases}$$

$$p = p(\rho, \varepsilon)F(\delta), \quad Y = Y_0F(\delta), \quad \mu = \mu_0F(\delta).$$

For copper, $\delta_1 = 0.95$, $\delta_2 = 0.9$. The initial conditions for the lining: $p = 0$, $S_{ik} = 0$, $\varepsilon = 0$, $u = 0$, $v = 0$, $\rho = \rho_0$, or u and v are assigned in the examples without regard for the explosive. The detonation of the explosive was calculated by the method in [13], which presumes that the form of the detonation wave and the parameters of the front are known and are equal to the parameters at the Jouguet point. A calculation was performed only for the detonation products between the front of the detonation wave and the surface bounding the dispersing detonation products. We took boundary conditions in the form $p = 0$ on all of the free surfaces, $S_{ik} = 0$ on the free surfaces of the lining, and $u_{n1} = u_{n2}$, $\sigma_r = 0$ on the explosive–lining contact surface (condition of free slip).

Main Elements of the Numerical Method. There are currently many numerical methods available for solving two-dimensional problems of mechanics. The method presented here is most similar to the "free particle" method [14]. At the initial moment of the calculation, we choose a certain number of fluid elements in accordance with the geometry of the object. In each element (point), we assign values to u, v, p, ρ, ε, and S_{ik} in accordance with the initial conditions. During the calculation, we follow the motion of these points and we calculate new values of pressure, velocity, etc. at them. The motion and the parameters of each element are determined on the basis of the state of the adjacent points. The adjacent points form an irregular local grid around each element. The grid is variable with respect to both space and time. The set of adjacent points should be based on the following assumptions: 1) the adjacent points form the closest neighborhood around the given point; 2) the angular distribution of the adjacent points is uniform to the extent possible; 3) the number of adjacent points is greater than four.

The principle on which the computational algorithm is based can be explained by taking the equation of motion as an example

$$\frac{du}{dt} = -\frac{1}{\rho}\frac{\partial p}{\partial r},$$

for which we can construct the following difference scheme:

$$u_{L,K}^{n+1/2} = u_{L,K}^{n} - \frac{1}{2}\Delta t \frac{1}{\rho_{L,K}^{n}}(pR)_{L,K}^{n}; \tag{2}$$

$$u_{L,K}^{n+1} = \tilde{u}_{L,K}^{n} - \Delta t \frac{1}{\rho_{L,K}^{n+1/2}}(pR)_{L,K}^{n+1/2}. \tag{3}$$

Here, (L, K) is the number of the element; $u_{L,K}{}^{n}$ is the velocity of the element at the moment t^n; $u_{L,K}{}^{n+1}$ is the velocity of the element at the moment t^{n+1}; $(pR)_{L,K}{}^{n}$ is the pressure gradient at the moment t^n. The term $\tilde{u}_{L,K}{}^{n}$ will be discussed below.

Calculation of the gradient $(pR)_{L,K}{}^{n}$ is particularly important. For the gradient, we assume that the points adjacent to the point (L, K) have the coordinates (r_i, z_i) and the

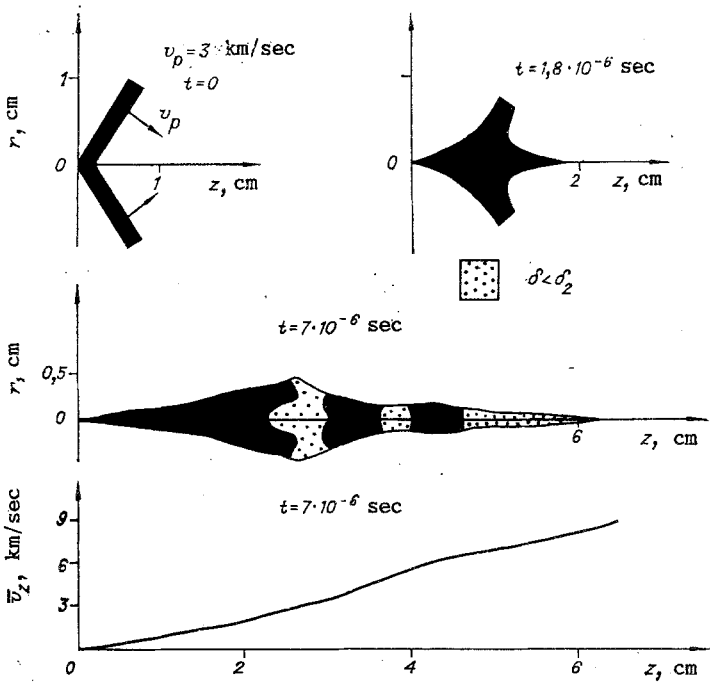

Fig. 2

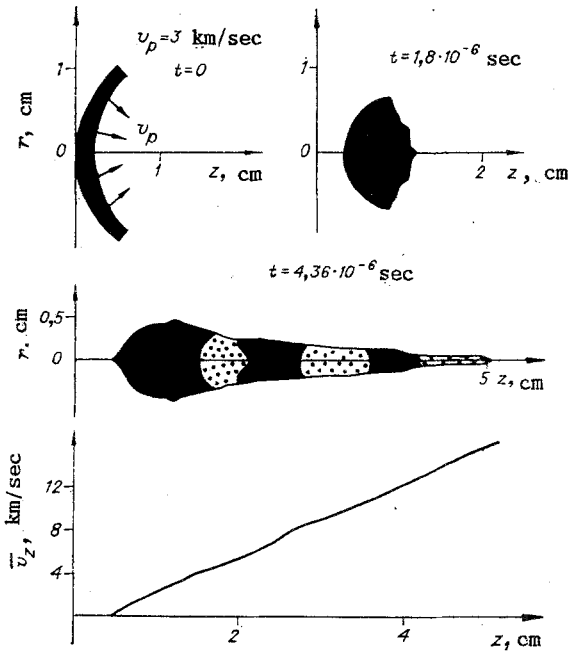

Fig. 3

pressure p_i. By means of linear interpolation between the point (L, K) and the adjacent points, we reduce the latter to a circle around the point (L, K). Now the interpolation points take the coordinates (r_i', z_i') and the pressure p_i'.

We assume that the pressure in the neighborhood of the point (L, K) is described by the formula

$$p(r, z) = p_0 + a(r - r_0) + b(z - z_0),$$

where r_0, z_0, and p_0 are the coordinates and pressure at the point (L, K). The values of and b are calculated by the least squares method:

$$\xi(a, b) = \sum_{i=1}^{N} [p_i' - p(r_i', z_i')]^2; \tag{4}$$

$$\frac{\partial \xi}{\partial a} = 0, \quad \frac{\partial \xi}{\partial b} = 0. \tag{5}$$

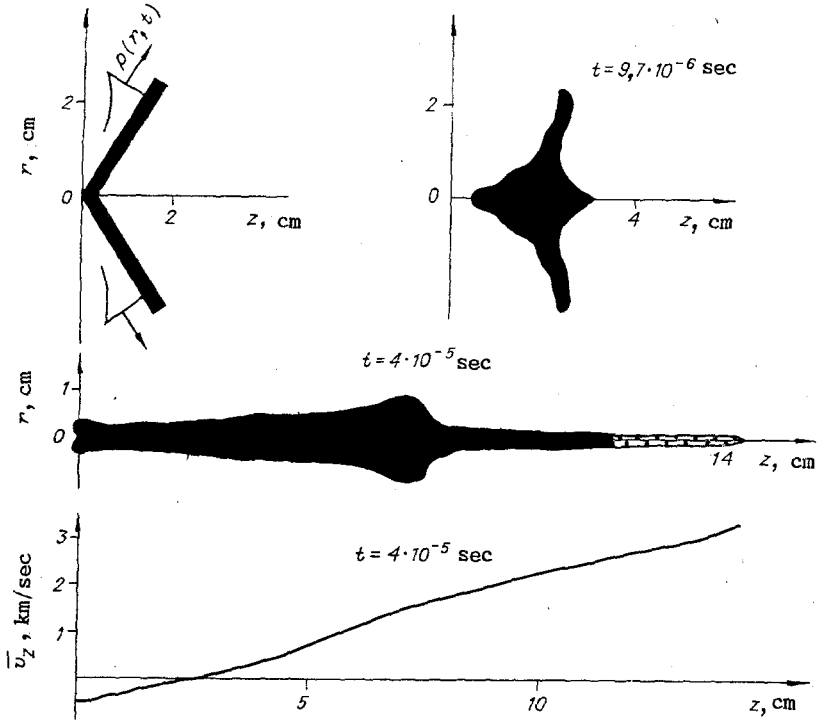

Fig. 4

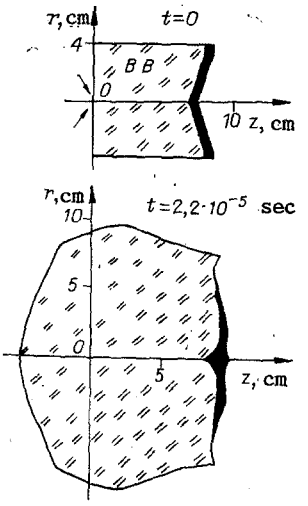

Fig. 5

We find a and b from Eqs. (5). Then

$$(pR)^n_{L,K} = a.$$

We similarly calculate all the of gradients, and then we calculate $v_{L,K}^{n+1}$, $\rho_{L,K}^{n+1}$, etc. We thus obtain new parameters for all of the theoretical points at the moment of time t^{n+1}. The expression for $\tilde{u}_{L,K}^{n}$ (3) can be represented in the form

$$\tilde{u}^n_{L,K} = u^n_{L,K} + \alpha(\bar{u}^n - u^n_{L,K})$$

(α = const Δt, $\bar{u}^n$ are the mean velocities of the adjacent points). The introduction of such an expression into the scheme means that we have added the numerical external diffusion, which damps numerical oscillations.

Sample Calculations. Figure 2 shows a sample solution of a problem of classical detonation. It is assumed that the lining has an initial velocity v_p which is directed perpendicular to the surface of the lining. The divergence angle of the lining is 120°. Also shown in Fig. 2 are three-dimensional sketches of the lining at selected moments of time and the distribution of mean velocity $\bar{v}_z$ along the z axis. The mass and velocity of the main part of the jet is consistent with the hydrodynamic theory of detonation. The high velocity of the small mass which forms the front part of the jet follows from the model assumption that the same velocity is specified along the r axis at all points at the initial moment of time (this includes points near the axis as well). Such a situation leads to the creation of a strong pressure pulse at the initial moment, this pulse corresponding to ejection of the small mass at a high velocity.

Figure 3 shows a similar example. The main difference is that the lining is spherical (S_{ik} = 0). It is evident that the detonation process is different in character than in the previous example. First, almost concentric compression takes place. Then mass is ejected from the center. The velocity of the jet increases monotonically over time, while in the preceding example it reached its maximum value at the beginning of the process. The calculations shown in Figs. 2-4 were the basis for constructing a complex numerical code in which we considered the effect of the explosive on the lining and the elastoplastic properties of the lining material. An example of such a solution is shown in Figs. 5-7. The divergence angle of the lining was made equal to 150° to allow us to simultaneously study the feasibility of using the numerical code to describe the phenomenon of inverse detonation.

Figure 5 shows the solution of a problem with so-called "sliding detonation." It was assumed here that the lining is accelerated by a pressure pulse with a prescribed space–time

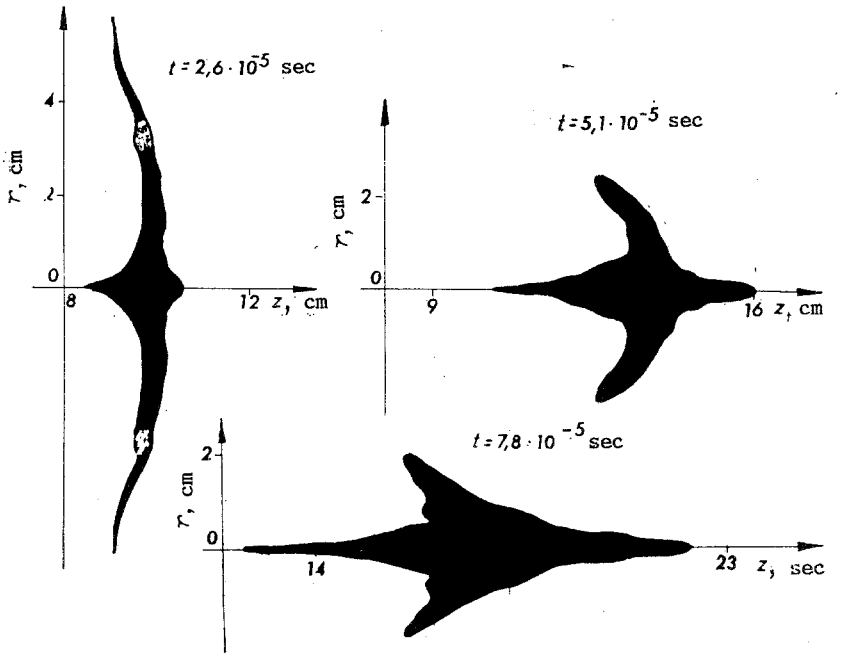

Fig. 6

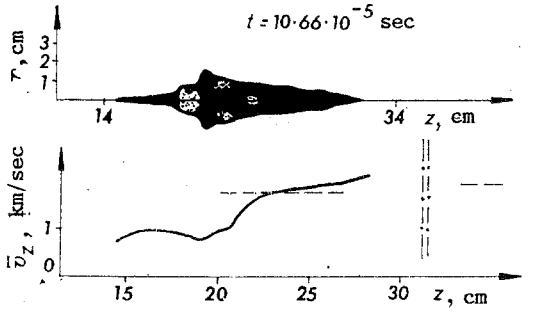

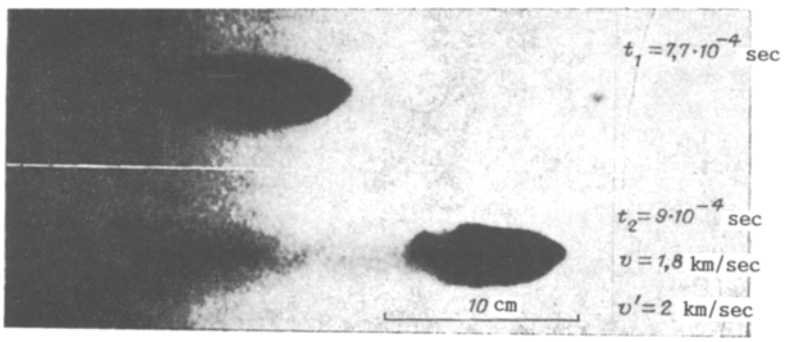

Fig. 7

profile. The pressure at the front of the pulse was assumed to be equal to the maximum value ($p_{max} = 0.5 \cdot 10^{11}$ Pa), while the detonation front moved at a velocity of 8 km/sec. It was also assumed that pressure behind the front fell in accordance with the formula

$$p = p_{max}\left[\frac{l}{l + D\tau}\right]^3, \quad l = 5 - \frac{5}{4} r_0, \quad \tau = t - t_0$$

(t_0 is the moment of time at which the front reaches the element with the radius r_0). The initial form of the lining and the explosive are shown in Fig. 5, which also shows the form of the detonation products and the lining at the moment of time 22 μsec. This is the moment at which the pressure of the detonation products is no greater than 10^9 Pa at any point. Thus, we no longer need consider the effect of the detonation products on the lining. At the

moment 26 μsec (Fig. 6), the first significant rupture of the medium is already visible ($\rho/\rho_0 < \delta_2$ in the entire region denoted by the points). The rupture region separates that part of the mass moving outside the symmetry axis from the part converging on the axis. With allowance for the fact that the description of the rupture region is only theoretical in character, we decided to divide the solution in two and will henceforth ignore that part of the shell which does not converge on the symmetry axis.

Figure 7 shows the final phase of the solution. This phase is marked by the beginning of significant rupture of the central part of the lining and the formation of a shaped charge. We were unable to perform calculations for later phases of the process, since we saw nonphysical behavior of the medium in the ruptured regions (particularly when secondary compression of the ruptured regions began).

Figure 7 also shows results of an experiment conducted by the shadow method (with an SNEF-4 camera) to evaluate this solution. The figure shows shadowgraphs (exposure to 40 nsec) of the already formed charge at the moments 770 and 900 μsec. The measured velocity of the charge was equal to 1.8 km/sec. Despite the fact that the theoretical calculation represents a phase of still unsteady motion, it can be concluded that: 1) satisfactory agreement is obtained between the theoretical and experimental charge velocities; 2) the graph of $\bar{v}_z(z)$ shows that the length of the charge is also in agreement with the experiment; 3) analysis of the stresses, velocity, and rupture regions indicates that a small mass may separate from the leading part of the charge (this can be seen in the first experimental photograph); 4) the diameter of the charge is greater in the experiment than in the calculation. This may be due to theoretical assumptions made regarding the properties of the medium, as well as to the deformation of the charge during rupture of the medium.

LITERATURE CITED

1. M. A. Lavrent'ev, "Principles of the functioning of a shaped charge," Usp. Mat. Nauk, 12, No. 4 (1957).
2. G. Birghoff et al., "Explosives with lined cavities," J. Appl. Phys., 19, No. 6 (1948).
3. V. M. Titov, "Possible regimes of hydrodynamic detonation with the collapse of the lining," Dokl. Akad. Nauk SSSR, 247, No. 5 (1979).
4. N. N. Gorshkov, "Use of hydrodynamic theory to describe the formation of a jet in inverse detonation," Fiz. Goreniya Vzryva, 19, No. 2 (1983).
5. S. A. Kinelovskii and Yu. A. Trishin, "Physical aspects of detonation," Fiz. Goreniya Vzryva, 16, No. 5 (1980).
6. N. A. Zlatin, "Limiting velocities of a continuous, condensed detonation jet," in: Problems of Mathematics and Mechanics [in Russian], Novosibirsk (1983).
7. P. C. Chou, J. Carleone, and R. R. Karpp, "Criteria for jet formation from impinging shells and plates," J. Appl. Phys., 47, No. 7 (1976).
8. N. Legrand and J. Ovadia, "Behavior of dense media under high dynamic pressures: Symposium" HDP, Paris (1978).
9. M. L. Wilkins, "Calculation of elastoplastic flows," Vychislitel'nyi Metody v Gidrodinamika, Moscow (1967).
10. A. I. Gulidov, V. M. Fomin, and N. N. Yanenko, "Numerical modeling of the penetration of bodies in an elastoplastic approximation," in: Problems of Mathematics and Mechanics [in Russian], Novosibirsk (1983).
11. K. P. Stanyukovich, Physics of Explosions [in Russian], Nauka, Moscow (1975).
12. G. Luttwak, Y. Kivity, and A. Abetzer, "Defect of a hypervelocity jet on a layered target," Int. J. Eng. Sci., 20, No. 8 (1982).
13. S. G. Sugak, G. I. Kanel', et al., "Numerical modeling of the effect of an explosion on an iron slab," Fiz. Goreniya Vzryva, 19, No. 2 (1983).
14. O. M. Belotserkovskii and Yu. M. Davydov, The Coarse-Particle Method in Gas Dynamics [in Russian], Nauka, Moscow (1982).